

Chapter 2

Optical Waveguide Modes

The optical waveguide is the fundamental element that interconnects the various devices of an optical integrated circuit, just as a metallic strip does in an electrical integrated circuit. However, unlike electrical current that flows through a metal strip according to Ohm's law, optical waves travel in the waveguide in distinct optical modes. A mode, in this sense, is a spatial distribution of optical energy in one or more dimensions that remains constant in time. In this chapter, the concept of optical modes in a waveguiding structure is discussed qualitatively, and key results of waveguide theory are presented with minimal proof to give the reader a general understanding of the nature of light propagation in an optical waveguide. Then, in Chap. 3, a mathematically sound development of waveguide theory is given.

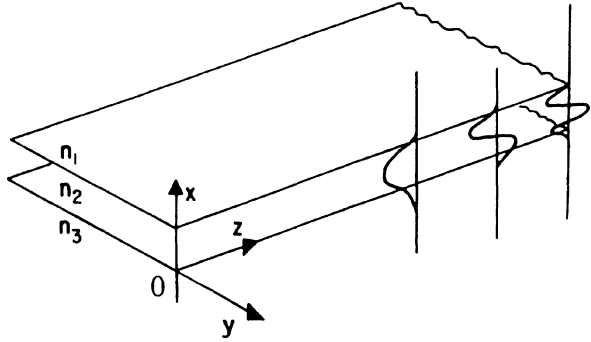
2.1 Modes in a Planar Waveguide Structure

As shown in Fig. 2.1, a planar waveguide is characterized by parallel planar boundaries with respect to one (x) direction, but is infinite in extent in the lateral directions (z and y). Of course, because it is infinite in two dimensions, it cannot be a practical waveguide for optical integrated circuits, but it forms the basis for the analysis of practical waveguides of rectangular cross section. It has therefore been treated by a number of authors, including McWhorter [1], McKenna [2], Tien [3], Marcuse [4], Taylor and Yariv [5] and Kogelnik [6]. In Section 2.1.2 we follow the approach of Taylor and Yariv [5] to examine the possible modes in a planar waveguide, without fully solving the wave equation.

2.1.1 Theoretical Description of the Modes of a Three-Layer Planar Waveguide

To begin the discussion of optical modes, consider the simple three-layer planar waveguiding structure of Fig. 2.1. The layers are all assumed to be infinite in extent in the y and z directions, and layers 1 and 3 are also assumed to be semi-infinite in the x direction. Light waves are assumed to be propagating in the z direction. It has

Fig. 2.1 Diagram of the basic three-layer planar waveguide structure. Three mode are shown, representing distributions of electric field in the x direction



been stated previously that a mode is a spatial distribution of optical energy in one or more dimensions. An equivalent mathematical definition of a mode is that it is an electromagnetic field which is a solution of Maxwell's wave equation

$$\nabla^2 \mathbf{E}(\mathbf{r}, t) = [n^2(\mathbf{r})/c^2] \partial^2 \mathbf{E}(\mathbf{r}, t) / \partial t^2, \quad (2.1)$$

where \mathbf{E} is the electric field vector, \mathbf{r} is the radius vector, $n(\mathbf{r})$ is the index of refraction, and c is the speed of light in a vacuum. For monochromatic waves, the solutions of (2.1) have the form

$$\mathbf{E}(\mathbf{r}, t) = \mathbf{E}(\mathbf{r}) e^{i\omega t}, \quad (2.2)$$

where ω is the radian frequency. Substituting (2.2) into (2.1) we obtain

$$\nabla^2 \mathbf{E}(\mathbf{r}) + k^2 n^2(\mathbf{r}) \mathbf{E}(\mathbf{r}) = 0, \quad (2.3)$$

where $k \equiv \omega/c$. If we assume, for convenience, a uniform plane wave propagating in the z direction, i.e., $\mathbf{E}(\mathbf{r}) = \mathbf{E}(x, y) \exp(-i\beta z)$, β being a propagation constant, then (2.3) becomes

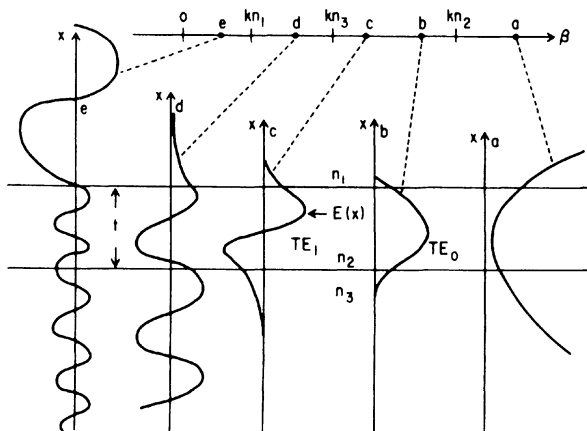
$$\partial^2 \mathbf{E}(x, y) / \partial x^2 + \partial^2 \mathbf{E}(x, y) / \partial y^2 + [k^2 n^2(\mathbf{r}) - \beta^2] \mathbf{E}(x, y) = 0. \quad (2.4)$$

Since the waveguide is assumed infinite in the y direction, by writing (2.4) separately for the three regions in x , we get

$$\begin{aligned} \text{Region 1} \quad & \partial^2 E(x, y) / \partial x^2 + (k^2 n_1^2 - \beta^2) E(x, y) = 0 \\ \text{Region 2} \quad & \partial^2 E(x, y) / \partial x^2 + (k^2 n_2^2 - \beta^2) E(x, y) = 0 \\ \text{Region 3} \quad & \partial^2 E(x, y) / \partial x^2 + (k^2 n_3^2 - \beta^2) E(x, y) = 0, \end{aligned} \quad (2.5)$$

where $E(x, y)$ is one of the Cartesian components of $\mathbf{E}(x, y)$. The solutions of (2.5) are either sinusoidal or exponential functions of x in each of the regions, depending

Fig. 2.2 Diagram of the possible modes in a planar waveguide [2.5]



on whether $(k^2 n_i^2 - \beta^2)$, $i = 1, 2, 3$, is greater than or less than zero. Of course, $E(x, y)$ and $\partial E(x, y)/\partial x$ must be continuous at the interface between layers. Hence the possible modes are limited to those shown in Fig. 2.2.

Consider how the mode shape changes as a function of β , for the case of constant frequency ω and $n_2 > n_3 > n_1$. This relative ordering of the indices is quite a common case, corresponding, for example, to a waveguiding layer of index n_2 formed on a substrate with smaller index n_3 , surrounded by air of index n_1 . As we will see in Chapter 3, it is a necessary condition for waveguiding in Layer 2 that n_2 be greater than both n_1 and n_3 . When $\beta > kn_2$, the function $E(x)$ must be exponential in all three regions and only the mode shape shown as (a) in Fig. 2.2 could satisfy the boundary conditions of $E(x)$ and $\partial E(x)/\partial x$ being continuous at the interfaces. This mode is not physically realizable because the field increases unboundedly in Layers 1 and 3, implying infinite energy. Modes (b) and (c) are well confined guided modes, generally referred to as the zeroth order and first order transverse electric modes, TE_0 and TE_1 [7]. For values of β between kn_2 and kn_3 such modes can be supported. If β is greater than kn_1 but less than kn_3 , a mode like that in (d) will result. This type of mode, which is confined at the air interface but sinusoidally varying at the substrate, is often called a *substrate radiation* mode. It can be supported by the waveguide structure, but because it is continually losing energy from the waveguiding Region 2 to the substrate Region 3 as it propagates, it tends to be damped out over at short distance. Hence it is not very useful in signal transmission, but, in fact, it may be very useful in coupler applications such as the tapered coupler. This type of coupler will be discussed in Chapter 6. If β is less than kn_1 the solution for $E(x)$ is oscillatory in all three regions of the waveguide structure. These modes are not guided modes because the energy is free to spread out of the waveguiding Region 2. They are generally referred to as the *air radiation* modes of the waveguide structure. Of course, radiation is also occurring at the substrate interface.

2.1.2 Cutoff Conditions

We shall see in Chapter 3, when (2.1) is formally solved, subject to appropriate boundary conditions at the interface, that β can have any value when it is less than kn_3 , but only discrete values of β are allowed in the range between kn_3 and kn_2 . These discrete values of β correspond to the various modes $TE_j, j = 0, 1, 2, \dots$ (or $TM_k, k = 0, 1, 2, \dots$). The number of modes that can be supported depends on the thickness t of the waveguiding layer and on ω, n_1, n_2 and n_3 . For given t, n_1, n_2 , and n_3 there is a cutoff frequency ω_c below which waveguiding cannot occur. This ω_c corresponds to a long wavelength cutoff λ_c .

Since wavelength is often a fixed parameter in a given application, the cutoff problem is frequently stated by asking the question, “for a given wavelength, what indices of refraction must be chosen in the three layers to permit waveguiding of a given mode?” For the special case of the so-called asymmetric waveguide, in which n_1 is very much less than n_3 , it can be shown (Chapter 3) that the required indices of refraction are related by

$$\Delta n = n_2 - n_3 = (2m + 1)^2 \lambda_0^2 / (32n_2 t^2), \quad (2.6)$$

where the mode number $m = 0, 1, 2, \dots$, and λ_0 is the vacuum wavelength. The change in index of refraction required for waveguiding of the lower-order modes is surprisingly small. For example, in a gallium arsenide waveguide with n_2 equal to 3.6 [8] and with t on the order of λ_0 , (2.6) predicts that a Δn on the order of only 10^{-2} is sufficient to support waveguiding of the TE_0 mode.

Because only a small change in index is needed, a great many different methods of waveguide fabrication have proven effective in a variety of substrate materials. The more important of these have been listed in Table 2.1 so that the reader will be familiar with the names of the techniques when they are mentioned in the following discussion of experimental observations of waveguide performance. A thorough explanation of the methods of waveguide fabrication is given in Chapters 4 and 5.

Table 2.1 Methods of fabricating waveguides for optical integrated circuits

-
- | | |
|----|--|
| 1) | Deposited thin films (glass, nitrides, oxides, organic polymers) |
| 2) | Photoresist films |
| 3) | Ion bombarded glass |
| 4) | Diffused dopant atoms |
| 5) | Heteroepitaxial layer growth |
| 6) | Electro-optic effect |
| 7) | Metal film stripline |
| 8) | Ion migration |
| 9) | Reduced carrier concentration in a semiconductor |
| | a) epitaxial layer growth |
| | b) diffusion counterdoping |
| | c) ion implantation counterdoping or compensation |
-

2.1.3 Experimental Observation of Waveguide Modes

Since the waveguides in optical integrated circuits are typically only a few micrometers thick, observation of the optical mode profile across a given dimension cannot be accomplished without a relatively elaborate experimental set-up, featuring at least $1000\times$ magnification. One such system [9], which works particularly well for semiconductor waveguides, is shown in Fig. 2.3. The sample, with its waveguide at the top surface, is fixed atop an x - y - z micropositioner. Microscope objective lenses, used for input beam coupling and output image magnification, are also mounted on micropositioners to facilitate the critical alignment that is required. The light source is a gas laser, emitting a wavelength to which the waveguide is transparent. For example, a helium-neon laser operating at $1.15\text{ }\mu\text{m}$ is good for GaAs, GaAlAs and GaP waveguides, while one emitting at $6328\text{ }\text{\AA}$ can be used for GaP but not for GaAlAs or GaAs. For visual observation of the waveguide mode, the output face of the waveguide can be imaged onto either a white screen or an image converter (IC) screen depending on whether visible wavelength or infrared (ir) light is used. The lowest order mode ($m = 0$) appears as a single band of light, while higher order modes have a correspondingly increased number of bands, as shown in Fig. 2.4.

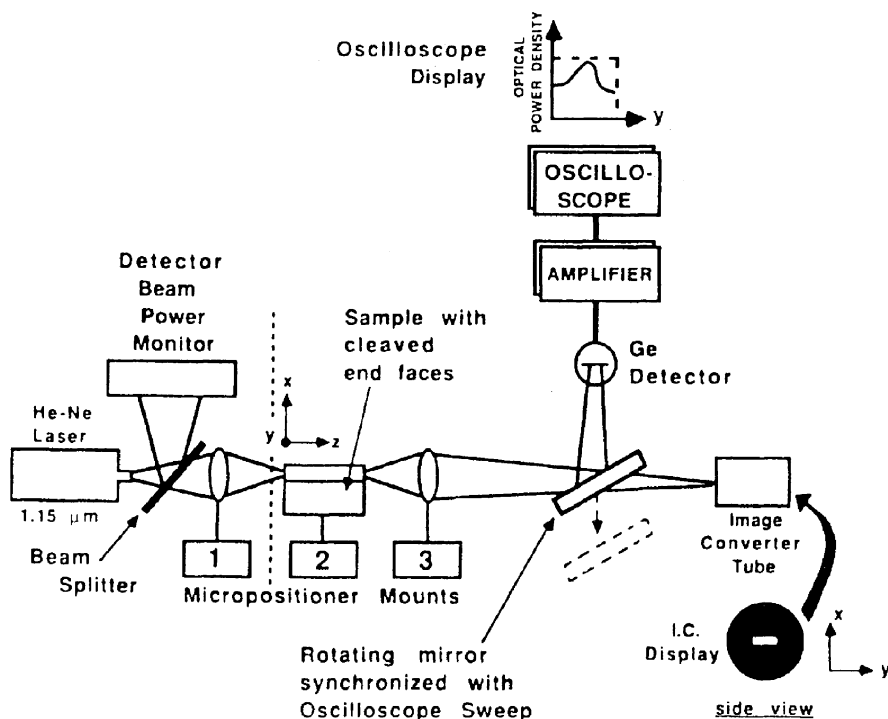


Fig. 2.3 Diagram of an experimental setup than can be used to measure optical mode shapes [2.9]

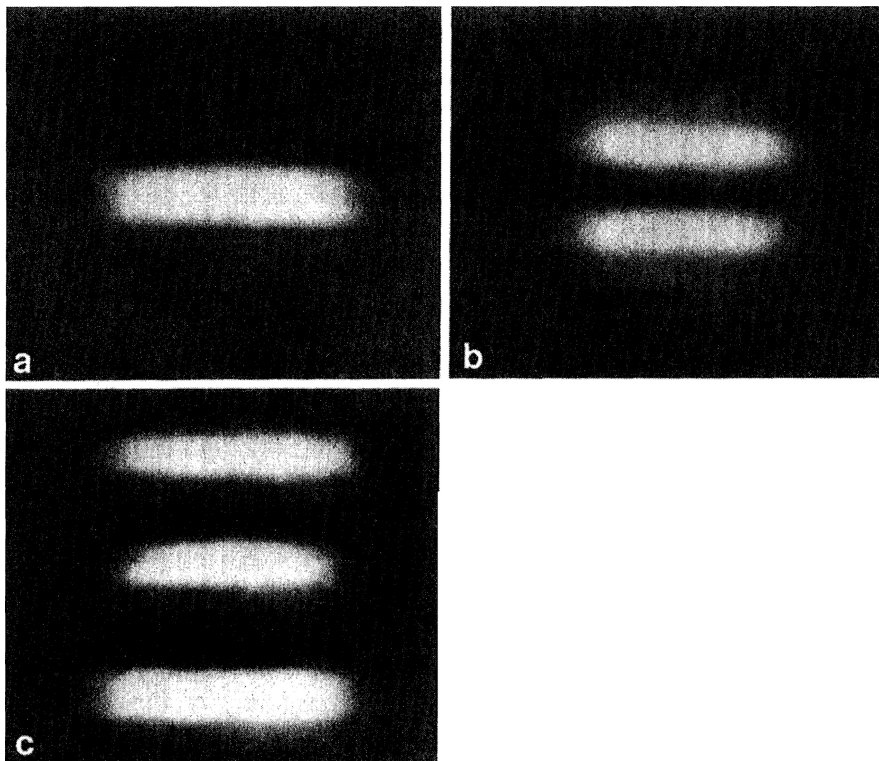


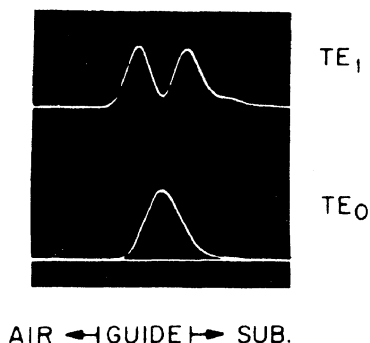
Fig. 2.4a, b, c Optical mode patterns in a planar waveguide, **a** TE_0 , **b** TE_1 , **c** TE_2 . In the planar guide, light is unconfined in the y direction, and is limited, as shown in the photos, only by the extent of spreading of the input laser beam. For the corresponding TE_{xy} patterns of a rectangular waveguide, see [10]

The light image appears as a band rather than a spot because it is confined by the waveguide only in the x direction. Since the waveguide is much wider than it is thick the laser beam is essentially free to diverge in the y direction.

To obtain a quantitative display of the mode profile, i.e. optical power density vs. distance across the face of the waveguide, a rotating mirror is used to scan the image of the waveguide face across a photodetector that is masked to a narrow slit input. The electrical signal from the detector is then fed to the vertical scale of an oscilloscope on which the horizontal sweep has been synchronized with the mirror scan rate. The result is in the form of graphic displays of the mode shape, like those shown in Fig. 2.5. Note that the modes have the theoretically predicted sinusoidal-exponential shape, by remembering that what is observed is optical power density, or intensity, which is proportional to E^2 . Details of the mode shape, like the rate of exponential decay (or extinction) of the evanescent “tail” extending across the waveguide-substrate and waveguide-air interfaces, depend strongly on the values of Δ at the interface. As can be seen in Fig. 2.5, the extinction is much sharper at

Fig. 2.5 Optical mode shapes are measured using the apparatus of Fig. 2.3. The waveguide in this case was formed by proton implantation into a gallium arsenide substrate to produce a $5\text{ }\mu\text{m}$ thick carrier-compensated layer [12]

TE₀ and TE₁ MODE PROFILES



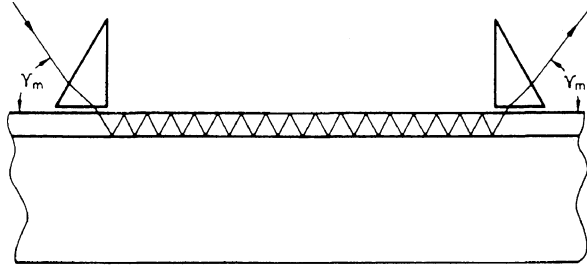
the waveguide-air interface where $\Delta n \simeq 2.5$ than at the waveguide-substrate plane where $\Delta n \simeq 0.01$ – 0.1 .

A system like that shown in Fig. 2.3 is particularly useful for analysis of mode shapes in semiconductor waveguides, which generally support only one or two modes because of the relatively small Δn at the waveguide-substrate interface. Generally, the position of the focused input laser beam can be moved toward the center of the waveguide to selectively pump the zeroth order mode, or toward either the air or substrate interface to select the first order mode. It becomes very difficult to visually resolve the light bands in the case of higher-order, multimode waveguides because of spatial overlapping, even though the modes may be electromagnetically distinct and non-coupled one to another. Waveguides produced by depositing thin films of oxides, nitrides or glasses onto glass or semiconductor substrates usually are multi-mode, supporting 3 or more modes, because of the larger waveguide-substrate Δn [11–14]. For waveguides of this type, a different experimental technique, employing prism coupling, is most often used to analyze the modes.

The prism coupler will be discussed in detail in Chapter 7. At this point it suffices to say that the prism coupler has the property that it selectively couples light into (or out of) a particular mode, depending on the angle of incidence (or emergence). The mode-selective property of the prism coupler, which is illustrated in Fig. 2.6, results from the fact that light in each mode within a waveguide propagates at a different velocity, and continuous phase-matching is required for coupling. The particular angle of incidence required to couple light into a given mode or the angle of emergence of light coupled out of a given mode can both be accurately calculated from theory, as will be seen in Chapter 7. The prism coupler can thus be used to analyze the modes of a waveguide. This can be done in two ways.

In one approach, the angle of incidence of a collimated, monochromatic laser beam on an input coupler prism is varied and the angles for which a propagating optical mode is introduced into the waveguide are noted. The propagation of optical energy in the waveguide can be observed by merely placing a photodetector at the

Fig. 2.6 The prism coupler used as a device for modal analysis



output end of the waveguide. One can then determine which modes the waveguide is capable of supporting by calculating from the angle of incidence data.

An alternative method uses the prism as an output coupler. In this case, monochromatic light is introduced into the waveguide in a manner so as to excite all of the waveguide modes. For example, a diverging laser beam, either from a semiconductor laser, or from a gas laser beam passed through a lens to produce divergence, is focused onto the input face of the waveguide. Since the light is not collimated, but rather enters the waveguide at a variety of angles, some energy is

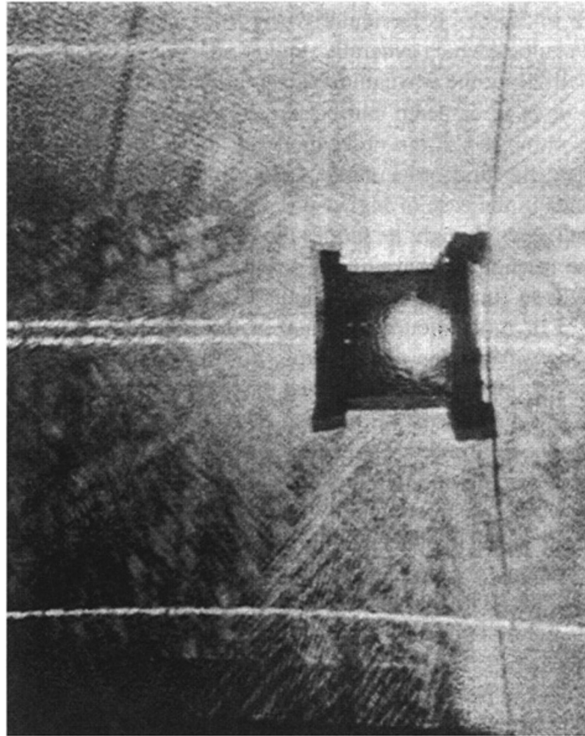


Fig. 2.7 Photograph of "m" lines produced by prism coupling of light out of a planar wave-guide. (Photo courtesy of U.S. Army ARRADCOM, Dover, NJ)

introduced into all of the waveguide modes for which the waveguide is above cutoff at the particular wavelength used. If a prism is then used as an output coupler, light from each mode emerges from the prism at a different angle. Again, the particular modes involved can be determined by calculation from the emergence angle data. Since the thickness of the waveguide is much less than its width, the emerging light from each mode appears as a band, producing a series of so-called “ m ” lines as shown in Fig. 2.7, corresponding to the particular mode number.

When the prism coupler is used to analyze the modes of a waveguide, the actual mode shape, or profile, cannot be determined in the same way as that of the scanning mirror approach of Fig. 2.3. However, the prism coupler method lets one determine how many modes can be supported by a multimode waveguide, and, as will be seen in Chap. 6, the phase velocity (hence the effective index of refraction) for each mode can be calculated from incidence and emergence angle data.

2.2 The Ray-Optic Approach to Optical Mode Theory

In Section 2.1, we considered the propagation of light in a waveguide as an electromagnetic field which mathematically represented a solution of Maxwell’s wave equation, subject to certain boundary conditions at the interfaces between planes of different indices of refraction. Plane waves propagating along the z direction, supported one or more optical modes. The light propagating in each mode traveled in the z direction with a different phase velocity, which is characteristic of that mode. This description of wave propagation is generally called the physical-optic approach. An alternative method, the so-called ray-optic approach [6, 15, 16, 17], is also possible but provides a less complete description. In this latter formulation, the light propagating in the z direction is considered to be composed of plane waves moving in zig-zag paths in the x - z plane undergoing total internal reflection at the interfaces bounding the waveguide. The plane waves comprising each mode travel with the same phase velocity. However, the angle of reflection in the zigzag path is different for each mode, making the z component of the phase velocity different. The plane waves are generally represented by rays drawn normal to the planes of constant phase as shown in Fig. 2.8, which explains the name *ray-optic*.

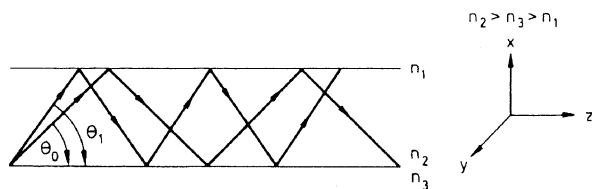


Fig. 2.8 Optical ray pattern within a multimode planar waveguide

2.2.1 Ray Patterns in the Three-Layer Planar Waveguide

The ray patterns shown in Fig. 2.8 correspond to two modes, say the TE_0 and TE_1 , propagating in a three layer waveguide with $n_2 > n_3 > n_1$. The electric (\mathbf{E}) and magnetic (\mathbf{H}) fields of these plane waves traveling along zig-zag paths would add vectorially to give the \mathbf{E} and \mathbf{H} distributions of the waves comprising the same two modes, propagating in the z direction, that were described by the physical-optic model of Section 2.1. Both the ray-optic and physical-optic formulations can be used to represent either TE waves, with components E_y , H_z , and H_x , or TM waves, with components H_y , E_z and E_x .

The correlation between the physical-optic and ray-optic approaches can be seen by referring back to (2.5). The solution to this equation in the waveguiding Region 2 has the form [2.5]:

$$E_y(x, z) \propto \sin(hx + \gamma), \quad (2.7)$$

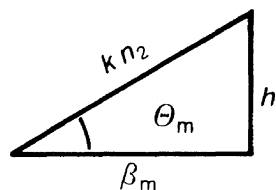
where a TE mode has been assumed, and where h and γ are dependent on the particular waveguide structure. Substituting (2.7) into (2.5) for Region 2, one obtains the condition

$$\beta^2 + h^2 = k^2 n_2^2. \quad (2.8)$$

Remembering that $k \equiv \omega/c$, it can be seen that β , h and kn_2 are all propagation constants, having units of $(\text{length})^{-1}$. A mode with a z direction propagation constant β_m and an x direction propagation constant h can thus be represented by a plane wave travelling at an angle $\theta_m = \tan^{-1}(h/\beta_m)$ with respect to the z direction, having a propagation constant kn_2 , as diagrammed in Fig. 2.9. Since the frequency is constant, $kn_2 \equiv (\omega/c)n_2$ is also constant, while θ_m , β_m and h are all parameters associated with the m th mode, with different values for different modes.

To explain the waveguiding of light in a planar three-layer guide like that of Fig. 2.8 by the ray-optic method, one needs only Snell's law of refraction, coupled with the phenomenon of total internal reflection. For a thorough discussion of these basic concepts of optics see, for example, *Condon* [18], or *Billings* [19], or *Benett* [20]. Consider a ray of light propagating within a three-layer waveguide structure as shown in Fig. 2.10. The light rays of Fig. 2.10a,b and c correspond to a radiation mode, a substrate mode, and a guided mode, respectively. The angles of incidence

Fig. 2.9 Geometric (vectorial) relationship between the propagation constants of an optical waveguide



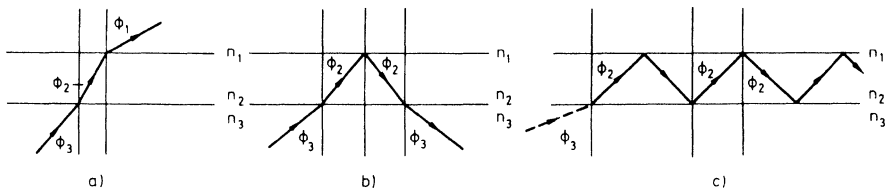


Fig. 2.10 a, b, c. Optical ray patterns for **a** air radiation modes; **b** substrate radiation modes; **c** guided mode. In each case a portion of the incident light is reflected back into layer 3; however, that ray has been omitted from the diagrams

and refraction, φ_i , with $i = 1, 2, 3$, are measured with respect to the normals to the interface planes, as is common practice in optics. From Snell's law

$$\sin \varphi_1 / \sin \varphi_2 = n_2 / n_1 \quad (2.9)$$

and

$$\sin \varphi_2 / \sin \varphi_3 = n_3 / n_2. \quad (2.10)$$

Beginning with very small angles of incidence, φ_3 , near zero, and gradually increasing φ_3 , we find the following behavior. When φ_3 is small, the light ray passes freely through both interfaces, suffering only refraction, as in Fig. 2.10a. This case corresponds to the radiation modes discussed in Section 2.1. As φ_3 is increased beyond the point at which φ_2 exceeds the critical angle for total internal reflection at the $n_2 - n_1$ interface, that light wave becomes partially confined as shown in Fig. 2.10b, corresponding to a substrate radiation mode. The condition for total internal reflection at the $n_2 - n_1$ interface is given by [19]

$$\varphi_2 \geq \sin^{-1}(n_1/n_2), \quad (2.11)$$

or, combining (2.11) and (2.10),

$$\varphi_3 \geq \sin^{-1}(n_1/n_3). \quad (2.12)$$

As φ_3 is further increased beyond the point at which φ_2 also exceeds the critical angle for total internal reflection at the $n_2 - n_3$ interface, the lightwave becomes totally confined, as shown in Fig. 2.10c, corresponding to a guided mode. In this case, the critical angle is given by

$$\varphi_2 \geq \sin^{-1}(n_3/n_2), \quad (2.13)$$

or, combining (2.2.7) and (2.2.4),

$$\varphi_3 \geq \sin^{-1}(1) = 90^\circ. \quad (2.14)$$

The conditions given by (2.11) and (2.13) for determining what type of modes can be supported by a particular waveguide as a function of φ_2 are exactly equivalent to the conditions given by (2.11) as a function of β . For example, (2.5) indicates that only radiation modes result for β less than kn_1 . Referring to Fig. 2.9, note that,

$$\varphi_2 = \beta/kn_2. \quad (2.15)$$

Thus, if $\beta \leq kn_1$,

$$\varphi_2 \leq kn_1/kn_2 = n_1/n_2, \quad (2.16)$$

which is the same condition given by (2.11). Similarly, if β is greater than kn_1 but less than kn_3 , (2.5) indicates that substrate radiation modes will be supported. Only when $\beta \geq kn_3$, can confined waveguide modes occur. From Fig. 2.9, if $\beta \geq kn_3$,

$$\sin \varphi_2 = \beta/kn_2 \geq kn_3/kn_2 \geq n_3/n_2. \quad (2.17)$$

Equation (2.17), obtained from physical-optic theory, is merely a repeat of (2.13) that resulted from the ray-optic approach. Finally, if β is greater than kn_2 ,

$$\sin \varphi_2 = \beta/kn_2 \geq 1. \quad (2.18)$$

Equation (2.18) is, of course, a physically unrealizable equality, corresponding to the physically unrealizable “a” type of modes of Fig. 2.2. Thus an equivalence has been demonstrated between the ray-optic and physical-optic approaches in regard to the determination of mode type.

2.2.2 The Discrete Nature of the Propagation Constant β

The correspondence between the ray-optic and physical optic formalisms extends beyond merely determining what type modes can be supported. It has been mentioned previously, and will be demonstrated mathematically in Chapter 3, that the solution of Maxwell’s equation subject to the appropriate boundary conditions requires that only certain discrete values of β are allowed. Thus, there are only a limited number of guided modes that can exist when β is in the range

$$kn_3 \leq \beta \leq kn_2. \quad (2.19)$$

This limitation on β can be visualized quite conveniently using the ray-optic approach. The plane wavefronts that are normal to the zig-zag rays of Fig. 2.8 are assumed to be infinite, or at least larger than the cross section of the waveguide that is intercepted; otherwise they would not fit the definition of a plane wave, which requires a constant phase over the plane. Thus, there is much overlapping of the waves as they travel in the zig-zag path. To avoid decay of optical energy due to

destructive interference as the waves travel through the guide, the total phase change for a point on a wavefront that travels from the $n_2 - n_3$ interface to the $n_2 - n_1$ interface and back again must be a multiple of 2π . This leads to the condition,

$$2kn_2t \sin \theta_m - 2\varphi_{23} - 2\varphi_{21} = 2m\pi, \quad (2.20)$$

where t is the thickness of the waveguiding Region 2, θ_m is the angle of reflection with respect to the z direction, as shown in Fig. 2.8, m is the mode number, and φ_{23} and φ_{21} , are the phase changes suffered upon total internal reflection at the interfaces. The phases $-2\varphi_{23}$ and $-2\varphi_{21}$, represent the Goos-Hänchen shifts [21, 22]. These phase shifts can be interpreted as penetration of the zig-zag ray (for a certain depth δ) into the confining layers 1 and 3 before it is reflected [6, pp. 25–29].

The values of φ_{23} and φ_{21} can be calculated from [22]:

$$\begin{aligned} \tan \varphi_{23} &= (n_2^2 \sin^2 \varphi_2 - n_3^2)^{1/2} / (n_2 \cos \varphi_2) \\ \tan \varphi_{21} &= (n_2^2 \sin^2 \varphi_2 - n_1^2)^{1/2} / (n_2 \cos \varphi_2) \end{aligned} \quad (2.21)$$

for TE waves, and

$$\begin{aligned} \tan \varphi_{23} &= n_2^2 (n_2^2 \sin^2 \varphi_2 - n_3^2)^{1/2} / (n_3^2 n_2 \cos \varphi_2) \\ \tan \varphi_{21} &= n_2^2 (n_2^2 \sin^2 \varphi_2 - n_1^2)^{1/2} / (n_1^2 n_2 \cos \varphi_2) \end{aligned} \quad (2.22)$$

for TM waves.

It can be seen that substitution of either (2.21) or (2.22) into (2.20) results in a transcendental equation in only one variable, θ_m , or φ_m , where

$$\varphi_m = \frac{\pi}{2} - \theta_m. \quad (2.23)$$

For a given m , the parameters n_1 , n_2 , n_3 and t , φ_m (or θ_m) can be calculated. Thus a discrete set of reflection angles φ_m are obtained corresponding to the various modes. However, valid solutions do not exist for all values of m . There is a cutoff condition on allowed values of m for each set of n_1 , n_2 , n_3 and t , corresponding to the point at which φ_m becomes less than the critical angle for total internal reflection at either the $n_2 - n_3$ or the $n_2 - n_1$ interface, as discussed in Section 2.2.1.

For each allowed mode, there is a corresponding propagation constant β_m given by

$$\beta_m = kn_2 \sin \varphi_m = kn_2 \cos \theta_m. \quad (2.24)$$

The velocity of the light parallel to the waveguide is then given by

$$v = c(k/\beta), \quad (2.25)$$

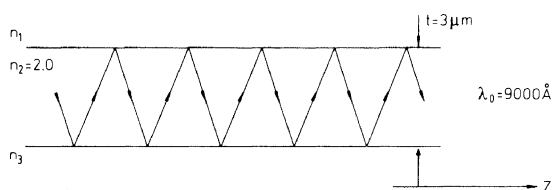
and one can define an effective index of refraction for the guide as

$$n_{\text{eff}} = c/v = \beta/k. \quad (2.26)$$

Chapter 2 has described the optical modes that can exist in a three-layer planar waveguide. We have seen that the modes can be described either by a physical-optic method, based on a solution of Maxwell's wave equation, or by a ray-optic method, relying on geometrical ray tracing principles of classical optics. In Chapter 3, the mathematical model underlying the mode theory will be developed in greater detail.

Problems

- 2.1 We wish to fabricate a planar waveguide in GaAs for light of wavelength $\lambda_0 = 1.1 \mu\text{m}$ that will operate in the single (fundamental) mode. If we assume a planar waveguide like that of Fig. 2.1 with the condition $n_2 - n_1 \gg n_2 - n_3$, what range of values can $n_2 - n_3$ have if $n_2 = 3.4$ and the thickness of the waveguiding layer $t = 3 \mu\text{m}$?
- 2.2 Repeat Problem 2.1 for the case $\lambda_0 = 1.06 \mu\text{m}$, all other parameters remaining unchanged.
- 2.3 Repeat Problems 2.1 and 2.2 for a waveguide of thickness $t = 6 \mu\text{m}$.
- 2.4 In a planar waveguide like that of Fig. 2.8 with $n_2 = 2.0$, $n_3 = 1.6$, and $n_1 = 1$, what is the angle of propagation of the lowest order mode (θ_0) when cutoff occurs? Is this a maximum or a minimum angle for θ_0 ?
- 2.5 Sketch the three lowest order modes in a planar waveguide like that of Fig. 2.8 with $n_1 = n_3 < n_2$.
- 2.6 A mode is propagating in a planar waveguide as shown with $\beta_m = 0.8 kn_2$. How many reflections at the $n_1 - n_2$ interface does the ray experience in traveling a distance of 1 cm in the z direction?



- 2.7 Show that the Goos-Hänchen phase shift goes to zero as the cutoff angle is approached for a waveguided optical mode.
- 2.8 Calculate the Goos-Hänchen shifts for a TE mode guided with $\beta = 1.85 k$ in a guide like that of Fig. 2.8, with $n_1 = 1.0$, $n_2 = 2.0$, $n_3 = 1.7$.
- 2.9 Show by drawing the vectorial relationship between the propagation constants (as in Fig. 2.9) How β , kn_2 and h change in relative magnitude and angle as one goes from the lowest-order mode in a waveguide progressively to higher-order modes.

- 2.10 A planar asymmetric waveguide is fabricated by depositing a $2\text{ }\mu\text{m}$ thick layer of Ta_2O_5 ($n = 2.09$) on to a quartz substrate ($n = 1.05$).
- How many modes can this waveguide support for light of $6328\text{ }\text{\AA}$ (vacuum wavelength)?
 - If a $20\text{ }\mu\text{m}$ layer of quartz ($n = 1.05$) is deposited on top of the Ta_2O_5 waveguide, how many modes can it support for light of $6328\text{ }\text{\AA}$ (vacuum wavelength)?
- 2.11 (a) Find the minimum required thickness for a planar slab waveguide with index of refraction $= 3.5$ on a substrate with index $= 3.38$ if it is to support the propagation of the lowest order TE mode of light with a vacuum wavelength 880 nm . The medium surrounding the waveguide and substrate is air.
- (b) If the thickness of the waveguide were increased above its minimum value by a factor of 2, and all other parameters remained unchanged, how many TE modes could be supported?

References

1. A. McWhorter: Solid State Electron. **6**, 417 (1963)
2. J. McKenna: Bell Syst. Techn. J. **46**, 1491 (1967)
3. P.K. Tien: Appl. Opt. **10**, 2395 (1971)
4. D. Marcuse: *Theory of Dielectric Optical Waveguides* (Academic, New York 1974)
5. H.F. Taylor, A. Yariv: IEEE Proc. **62**, 1044 (1974)
6. H. Kogelnik: Theory of dielectric waveguides, in *Integrated Optics*, T. Tamir (ed.), 2nd edn., Topics Appl. Phys., Vol. 7 (Springer, Berlin, Heidelberg 1979) Chap. 2
7. A. Yariv: *Optical Electronics in Modern Communications*, 5th edn. (Oxford University Press, New York, Oxford 1997) Chap. 13
8. D.T.F. Marple: J. Appl. Phys. **35**, 1241 (1964)
9. E. Garmire, H. Stoll, A. Yariv, R.G. Hunsperger: Appl. Phys. Lett. **21**, 87 (1972)
10. J. Goell: Bell Syst. Tech. J. **48**, 2133 (1969)
11. P.K. Tien, G. Smolinsky, R.J. Martin: Appl. Opt. **11**, 637 (1972)
12. D.H. Hensler, J. Cuthbert, R.J. Martin, P.K. Tien: Appl. Opt. **10**, 1037 (1971)
13. R.G. Hunsperger, A. Yariv, A. Lee: Appl. Opt. **16**, 1026 (1977)
14. Y. Luo, D.C. Hall, L. Kou, O. Blum, H. Hou, L. Steingart, J.H. Jackson: Optical Properties of $\text{Al}_x\text{Ga}_{(1-x)}\text{As}$ heterostructure native oxide planar waveguides. LEOS'99, IEEE Lasers and Electro-Optics Society 12th Annual Meeting, Orlando, Florida (1999)
15. R. Ulrich, R.J. Martin: Appl. Opt. **10**, 2077 (1971)
16. S.J. Maurer, L.B. Felsen: IEEE Proc. **55**, 1718 (1967)
17. H.K.V. Lotsch: Optik **27**, 239 (1968)
18. E.U. Condon: Electromagnetic waves, in *Handbook of Physics*, (ed.) E.U. Condon H. Odishaw (eds.) (McGraw-Hill, New York 1967) pp. 6–8
19. B.H. Billings: Optics, in *American Institute of Physics Handbook*, D.E. Gray, 3rd edn. (McGraw-Hill, New York 1972) pp. 6–9
20. H.E. Bennett: Reflection, in *The Encyclopedia of Physics*, (ed.) R.M. Besancon 3rd edn. (Van Nostrand Reinhold, New York 1990) pp. 1050–51
21. H.K.V. Lotsch: Optik **32**, 116–137, 189–204, 299–319, 553–569 (1970/71)
22. M. Born, E. Wolf: *Principles of Optics*, 3rd edn. (Pergamon, New York 1970) p. 49



<http://www.springer.com/978-0-387-89774-5>

Integrated Optics

Theory and Technology

Hunsperger, R.

2009, XXVIII, 513 p. 300 illus., Hardcover

ISBN: 978-0-387-89774-5